Macromolecules

Volume 37, Number 3 February 10, 2004

Communications to the Editor

Elimination of Extrudate Distortions in Metallocene-Catalyzed Polyethylene

M. Aguilar, M. T. Expósito, J. F. Vega, A. Muñoz-Escalona, and J. Martínez-Salazar*

Departamento de Física Macromolecular, Instituto de Estructura de la Materia, CSIC, Serrano113-123, 28006 Madrid, Spain

Received August 10, 2003
Revised Manuscript Received December 19, 2003

The elimination of extrudate distortions in polymers has been the topic of a number of studies. Attempts made to minimize surface roughness in polymer processing include using specially designed capillary dies,[1] blending with specific chemicals,[2] and processing at temperatures just above the melting point.[3] Besides these measures, methods such as modifying the molecular structure of the polymer itself have proved successful in eliminating irregularities. Altering the polymer's molecular structure involves the introduction of long chain branching by the use of single-site catalyst (SSC) systems in polymerization.[4] However, the intrinsic mechanism whereby distortions disappear has not yet been established. There is clear disagreement between authors who propose a molecular slip-stick mechanism for the removal of defects at the polymer/wall interface[5] and those who argue that extensional deformation of the molten polymer surface at the capillary exit is reduced.[6]

In this report, we present our preliminary results on the use of small amounts of ultrahigh molecular weight polyethylene (UHMWPE) as a possible route for the elimination of distortions in metallocene polyethylenes (mPEs). We evaluated the morphological, thermal properties, melt linear viscoelastic response, and capillary flow behavior of blends of an ethylene/1-hexene copolymer (Repsol YPF) obtained through an SSC system and the UHMWPE, HI-ZEX 240 M (Mitsui Chemicals America, Inc.). The copolymer has a weight-average molecular weight, M_w, of 118×10^3, a polydispersity index, M_w/M_n, of 2.2, and a branching content (butyl) of 10.7 CH_3/1000 C atoms. The molecular weight of the UHMWPE is close to 4.5×10^6. The characterization methods used have been described elsewhere[3]. The relative percentage weights of the mPE in the mPE/UHMWPE blend were 99.5 and 98.5. We first dissolved both polymers at high temperature in the presence of antithermooxidative degradation agents for a period of at least 1 h. The mixed system was then precipitated by adding a nonsolvent, dried, and compression molded at 180 °C for 5 min.

The spherulitic morphology of the samples was evaluated by polarized light microscopy using a Nikon Eclipse E600POL equipped with a digital camera DXM1200 and a Metler FT82 hot stage. A Perkin-Elmer DSC was used for the thermal analysis and indium was used as a calibration standard. The melting thermograms were recorded at heating rates of 10, 20, and 40 °C/min. Small-amplitude oscillatory measurements in the linear viscoelastic region were also performed in a controlled-stress rheometer across broad angular frequency and temperature ranges. The pure linear mPE material and the mixtures were also subjected to capillary extrusion using a piston-type rheoscope over a wide range of shear rates. The melt temperature was maintained at 160 °C during extrusion. Individual extrudate samples were collected and photographed.

The spherulitic morphology of the mPE was unaltered by the presence of the UHMWPE. Neither did its radial growth or size seem to be affected by the UHMWPE. Further, we detected no inclusion of separate regions of material. By DSC analysis of the samples, it was established that the UHMWPE does not form a separate crystalline phase (see Figure 1). However, for a more accurate analysis of the onset of the main melting peak recorded at different heating rates, one could appreciate a small delay in the annealing mechanism during heating. The inset in Figure 1 shows a plot of the

* Corresponding author. E-mail: jmsalazar@iem.cfmac.csic.es. Telephone: +34 915901618. Fax +34 915855413.

10.1021/ma035173y CCC: $27.50
Published on Web 01/16/2004

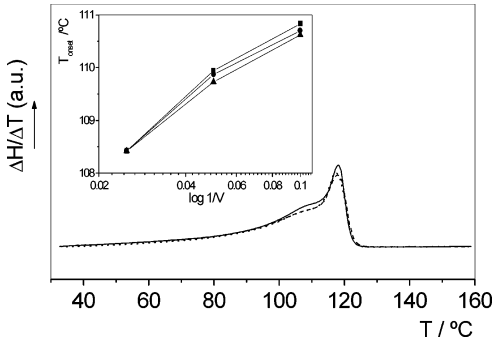

Figure 1. Melting endotherms for the mPE (continuous line) and the mPE/UHMWPE blends: 99.5/0.5 (dotted line) and 98.5/1.5 (dashed line) at a heating rate of 40 °C/min. The inset figure is the plot of the melting temperature onset vs the log of the reciprocal of the heating rate.

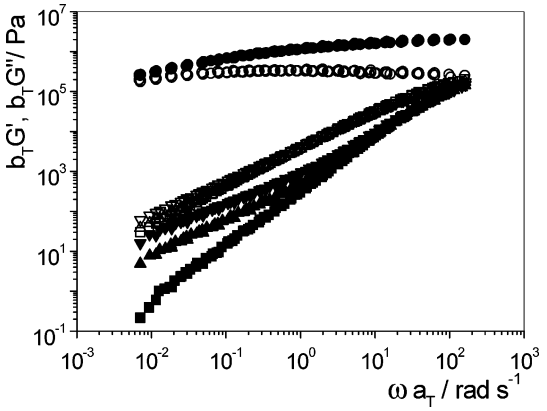

Figure 2. Master curves of the storage modulus, G' (close symbols), loss modulus, G'' (open symbols), vs the normalized angular frequency, ωa_T, at $T_o = 190$ °C for the mPE (■, □) and UHMWPE (●, ○) and the mPE/UHMWPE blends: 99.5/0.5 (▲, △); 98.5/1.5 (▼, ▽)

melting temperature onset against the reciprocal of the heating rate for the matrix and the two blends. As the UHMWPE is added, the slope decreases systematically. Moreover, there is also a concurrent decrease in the total enthalpy of matrix melting (5 and 7% for the samples 99.5/0.5 and 98.5/1.5, respectively). The overall picture indicates then that the two polymers intimately mix at the molecular level.

The data obtained in oscillatory shear at different temperatures were shifted at a reference temperature $T_o = 190$ °C defining the shift factors, a_T and b_T, for the frequency and the modulus, respectively. Superpositioning of results was excellent.

Figure 2 shows a clear difference in the viscoelastic moduli, G' and G'', of the pure materials and blends. The broad "plateau" region shown by the UHMWPE is the result of the large number of entanglements per molecule. It was impossible to reach the terminal region at very low frequencies, most probably due to the high M_w of the sample. The mPE showed the characteristic response of a linear polymer, and closely followed the well-known dependencies for the storage modulus, $G' \propto \omega^2$, and the loss modulus, $G'' \propto \omega$, at low frequencies. As UHMWPE is introduced into the matrix, its elastic character is enhanced, reflected by the upward concave shape of G' at low frequencies. This specific feature might be attributable to a long relaxation time component due to the UHMWPE. Similar results were recently obtained in homogeneous dispersions of UHMW polystyrene (PS) in PS across the composition range

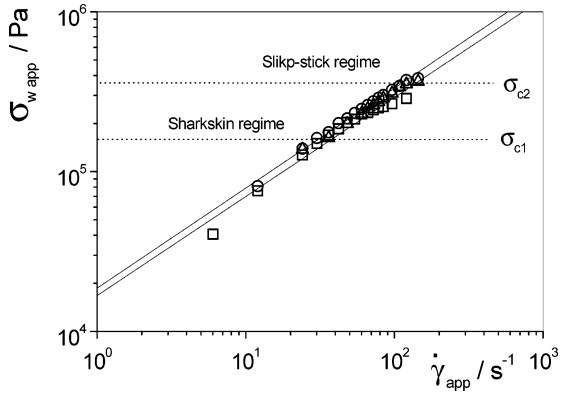

Figure 3. Flow curves at 160 °C for the mPE (□) and for the two blends examined: 99.5/0.5 (○); 98.5/1.5 (△). Dashed lines represent the critical values of the apparent shear stress for the onset of distortion regimes for the pure mPE sample. Solid lines represent the power law fit of the data (see text for details)

0.1−1% UHMWPS.[7] The upward tendency observed in the elastic function could be related to the presence of a deformable dispersed phase. However, in this specific case, the rise in G' should occur in the extremely low-frequency modulus zone, since the deformation process is one of very high viscosity inclusions.[8] At this point, we could suspect that UHMWPE is in fact homogeneously incorporated in the matrix. Dumoulin et al.[9] also found that a fraction of UHMWPE could be effectively incorporated in the PE matrix although in that case most of the material remained as inclusions.

The values of the extrusion apparent wall shear stress, $\sigma_{w,app}$, vs apparent shear rate, $\dot{\gamma}_{app}$, at 160 °C are shown in Figure 3. For the three samples, the mPE and the blends, the well-known power-law equation, $\sigma_{w,app} = K\dot{\gamma}_{app}^{n}$, holds. A similar power law exponent $n \approx 0.70$ was found in the apparent shear rate range 1−100 s^{-1} in all the samples. This means that shear thinning behavior is not substantially enhanced by the addition of low amounts of high-M_w species to the mPE. The sharkskin regime, characterized by high frequency, small-amplitude periodic distortions across the extrudate surface, was observed in the mPE once a critical value of shear stress of about $\sigma_{wc1} = 0.16$ MPa was reached. This value is well inside the range 0.1−0.2 MPa found for linear mPE.[10] A second distortion regime at a shear stress of about $\sigma_{wc2} = 0.37$ MPa was also noted. At this critical value, the slip-stick transition characterized by sudden oscillations in the extrusion pressure and the appearance of alternatively smooth and rough extrudates takes place. In this case, it is assumed that beyond the critical shear stress, σ_{wc2}, a large slip of the material along the die wall occurs.[10]

Morphological details of the cooled extrudates obtained in the sharkskin region, such as those shown in Figure 4, were analyzed for the pure mPE and blends studied. The extrudates were collected at 160 °C under similar conditions of shear stress, $\sigma_{w,app} \approx 0.30$ MPa, just before the slip-stick transition. It can be observed that for pure mPE, the sharkskin distortion is a periodic helix. However, for the blends, defects on the extrudate surface vanished, even at the lowest UHMWPE content. It should be underscored that this effect occurs at extrusion pressures within the limits of sharkskin and slip-stick transitions (0.16−0.37 MPa, see Figure 3) and is not accompanied by increased shear thinning. In addition, the blends show a conspicuous extrudate die-

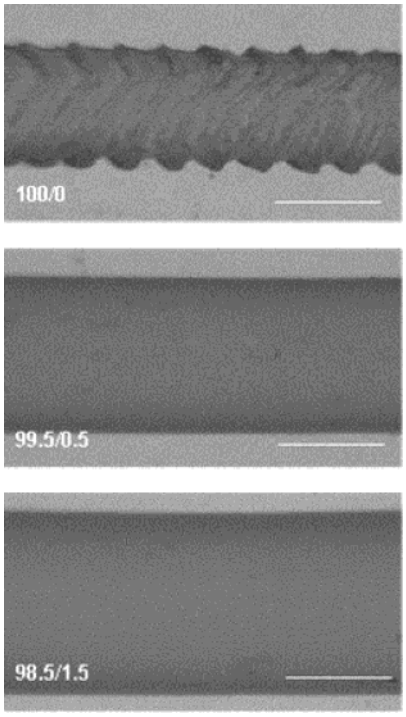

Figure 4. Micrographs of extrudates of the mPE and blends obtained at $T = 160$ °C for similar values of wall shear stress, $\sigma_{w,app} \approx 0.30$ MPa. The bar represents 1 mm.

swell, suggesting a considerably enhanced elastic character.

We may conclude that the cause of the lack of distortion is the presence of low amounts of very high-M_w species. According to the theory based on the interfacial molecular instability model,[5] these species might delay the entanglement-disentanglement transition causing the distortions as a consequence of a greater overall relaxation time of the blend. During flow along the die, very long molecules are stretched in the flow direction, possibly suppressing the coil−stretch oscillating mechanism causing chain disentanglement and the sharkskin effect. The fact that the addition of UHMWPE slightly increases the pressure in the sharkskin region may indicate that there is not slip at the polymer−wall interface. Alternatively, the elimination of distortion could also be explained by the model of cohesive failure by extensional deformation developed by Migler and co-workers.[6] On the basis of the ideas of Cogswell,[11] these authors recently suggested that sharkskin is caused by the tearing of the polymer due to the high extensional strain rate to which the material is subjected, just past the exit at the polymer−air interface. Hence, the factor controlling the onset of distortion is the product of the extensional strain rate, $\dot{\epsilon}$, and the total strain, T ($\dot{T} = \dot{\epsilon}T$), the *reconfiguration time*. It has been shown, that distortion appears when a critical value of the *reconfiguration time* is reached. It is obvious that if the melt strength of the material is increased, the extensional deformation at a given extrudate velocity at the exit should decrease. Thus, the critical value of the *reconfiguration time* for the tearing of the extrudate could not be reached. Indeed, there are no distortions in branched polymers such as low-density polyethylene (LDPE) and ethylene−vinyl acetate (EVA) copolymers,[12] in which chain branching is generally considered to delay chain dynamics and enhance elasticity and extensional viscosity.[13] Small amounts of high-M_w material in linear polymers have been described to cause extensional strain hardening[14] induced by the increased relaxation time.[7] Further investigations designed to explore the rheological behavior of a wide range of blend compositions and alternative mixing methods are currently in progress.

Acknowledgment. Thanks are due to the MICYT (Grant MAT2002-01242) for supporting this investigation. M.A. was awarded a post-graduate fellowship by the E.S.F. I3P program (2003). M.T.E. is a holder of a Ph.D. grant from the MICYT.

References and Notes

(1) Piau, J. M.; Nigen, S.; El Kissi, N. *J. Non-Newtonian Fluid Mech.* **2000**, *91*, 37−57.
(2) Rosenbaum, E. E.; Randa, S. K.; Hatzikiriakos, S. G.; Stewart, C. W.; Henry, D. L.; Buckmaster, M. *Polym. Eng. Sci.* **2000**, *40*, 179−190.
(3) Aguilar, M.; Vega, J. F.; Muñoz-Escalona, A.; Martínez-Salazar, J. *J. Mater. Sci.* **2002**, *37*, 3415−3421.
(4) Kim, Y. S.; Chung, C. I.; Lai, S. Y.; Hyun, K. S. *J. Appl. Polym. Sci.* **1996**, *59*, 125−137.
(5) Wang, S. Q.; Drda, P. A. *Macromol. Chem. Phys.* **1997**, *189*, 673−701.
(6) Migler, K. B.; Son, Y.; Qiao, F.; Flynn, K. *J. Rheol.* **2002**, *46*, 383−400.
(7) Minegishi, A.; Nishioka, A.; Takahashi, Y.; Masubuchi, Y.; Takimoto, J.-I.; Koyama, K. *Rheol. Acta* **2001**, *40*, 329−338.
(8) Graebling, D.; Muller, R.; Palierne, J. F. *Macromolecules* **1993**, *26*, 320−329.
(9) Dumoulin, M. M.; Utracki, L. A.; Lara, J. *Polym. Eng. Sci.* **1984**, *24*, 117−126.
(10) Denn, M. M. *Annu. Rev. Fluid Mech.* **2001**, *33*, 265−287.
(11) Cogswell, F. N.; Barone, J. R.; Plucktaveesak, N.; Wang, S. Q. *J. Rheol.* **1999**, *43*, 245−252.
(12) Yang, X.; Ishida, H.; Wang, S. Q. *J. Rheol.* **1998**, *42*, 63−80.
(13) Münstedt, H.; Laun, H. M. *Rheol. Acta* **1981**, *20*, 211−221.
(14) Münstedt, H. *J. Rheol.* **1980**, *24*, 847−867.

MA035173Y